Centre for Computational Finance and Economic Agents

WP071-13

Working Paper Series

Iacopo Giampaoli
Wing Lon Ng
Nick Constantinou

Periodicities of Foreign Exchange Markets and the Directional Change Power Law

2013

University of Essex

CCFEA
Centre for Computational Finance and Economic Agents

Periodicities of Foreign Exchange Markets and the Directional Change Power Law

Iacopo Giampaoli * Wing Lon Ng† Nick Constantinou ‡

April 11, 2013

Abstract

This paper utilises advanced methods from Fourier Analysis in order to describe periodicities in financial ultra-high frequent FX data. The Lomb-Scargle Fourier transform is used to take into account the irregularity in spacing in the time-domain. It provides a natural framework for the power spectra of different inhomogeneous time series processes to be easily and quickly estimated. Furthermore, event-based approach in intrinsic time based on a power-law relationship, is employed using different event thresholds to filter the foreign exchange tick-data. The calculated spectral density demonstrates that the price process in intrinsic time contains different periodic components for directional changes, especially in the medium-long term, implying the existence of stylised facts of ultra-high frequency data in the frequency domain.

Keywords: Ultra-high frequency transaction data, foreign exchange, irregularly spaced data, Lomb-Scargle Fourier transforms, spectral density.

JEL Classifications: C22, C58, C63.

*Centre for Computational Finance and Economic Agents (CCFEA), University of Essex, Wivenhoe Park, Colchester CO4 3SQ, UK.

†**Corresponding author**. E-mail: wlng@essex.ac.uk. Centre for Computational Finance and Economic Agents (CCFEA), University of Essex, Wivenhoe Park, Colchester CO4 3SQ, UK.

‡Essex Business School, University of Essex, Wivenhoe Park, Colchester CO4 3SQ, UK.

The authors are grateful to Richard Olsen for his valuable helpful discussion and to Olsen Financial Technologies for providing the FX market data.

1 Introduction

In financial markets, trading activity typically tends to vary depending on the time of day, shrinking during lunch time and over weekends, and increasing prior to major scheduled news announcements (see, for example, Chordia, Roll, and Subrahmanyam, 2001). These observations are usually measured in *physical time*. Another approach that has been recently put forward and which has led to a rich array of scaling behaviour in FX market is a time scale that is defined via events, i.e. the so called *intrinsic time* (see Derman, 2002; Glattfelder, Dupuis, and Olsen, 2011).

In particular, the presence of different patterns of trading activity in financial markets makes the flow of physical time discontinuous, as the number of transactions tends to increase or decrease at different time intervals. This empirical observation, which led to the definition of intrinsic "trading time", coined by Mandelbrot and Taylor (1967), suggests that the concept of physical time may not be the fundamental time scale and research should additionally focus on an event-based time scale. In this paper, the analysis of price movements focuses on an intrinsic time scale defined by "directional-change" events: price movements exceeding a given threshold which are independent of the notion of physical time. Recent literature has demonstrated a rich landscape of scaling laws in intrinsic time for "ultra-high-frequency" (UHF) FX data (for an early survey, see Bouchaud (2001, 2002)), including a scaling law for the directional-change events considered in this paper.

Following the intrinsic time paradigm by Glattfelder, Dupuis, and Olsen (2011), we filter our UHF data by analysing those points where there has been a directional-change (the *event*), consisting of price movements away from a local maximum (or minimum), which exceed a given threshold (for a more formal description, see Hautsch, 2004, p. 36). The newly created time series naturally includes fewer observations, but still contains significant information about the price evolution via its associated scaling law and about the temporal structures through its directional-change duration, and is irregular-spaced in time. Indeed, time series in intrinsic

time are fundamentally unevenly-spaced in time and there is no justification in artificially making them equally-spaced (see also Dacorogna, Gençay, Müller, Olsen, and Pictet, 2001; Giampaoli, Ng, and Constantinou, 2009).

Aldridge (2010) argues that trading opportunities are indeed present at various data frequencies (i.e. observation intervals), hence suggesting that agents with different time horizons and risk preferences would be able to trade profitably in the market. One of the key features common to all types of high-frequency data is the persistence of underlying trading opportunities: these range from fractions-of-a-second price movements, arising from market-making trades, to several-minute-long strategies based on momentum forecasted by microstructure theories, to several-hour-long market moves deriving from cyclical events and deviations from statistical relationships (Aldridge, 2010). The development of high-frequency trading strategies begins with the identification of *recurrent* (i.e. periodic) profitable trading opportunities present in the data, and their profitability depends upon the chosen trading frequency. As the data frequency increases, the possible range of each price movement shrinks, but the number of ranges increases, thus potentially increasing trades profitability [1].

The main goal of this paper is to detect potential periodic patterns of UHF FX market data. For example, it is well-known that intraday data have a consistent diurnal pattern of trading activities over the course of a trading day due to institutional characteristics of organised financial markets, such as opening and closing hours or intraday auctions. In fact, FX markets have stronger seasonal patterns as they are open 24/7 and constantly influenced by re-occurring time-zone effects. (see also Bauwens, Ben Omrane, and Giot, 2005; Ben Omrane and de Bodt, 2007).

In particular, this paper employs advanced modelling techniques from Fourier analysis, which provide a natural framework to analyse inhomogeneous time series

[1] In fact, Aldridge (2010) calculates the maximum gain as the sum of price ranges at each frequency, whereas the maximum potential gain (loss) at every frequency is determined by the (negative) sum of all per-period ranges at that frequency.

in the frequency domain and also reduce the computational time needed to process a large amount of transaction data. Fast Fourier transform (FFT) algorithms are commonly used to analyse equally-spaced time series in the frequency domain, but in their standard form, they require either regular resampling of the unevenly-spaced data, or interpolating them onto an equally-spaced grid (Bisig, Dupuis, Impagliazzo, and Olsen, 2012). In fact, any such transformation via regular resampling of unevenly-spaced data or interpolation to an evenly-spaced grid (in order to calculate the SDF with the simple FFT), leading to loss of information and the use of spurious information (Giampaoli, Ng, and Constantinou, 2009).

The Lomb-Scargle Fourier transform (LSFT), a generalisation of the discrete Fourier transform, is especially designed for unevenly-spaced data and represents the natural tool to study UHF data in the frequency domain as it allows the stochastic behaviour of every single process to be determined without any loss of information. The LSFT, in contrast to existing autoregressive conditional models (e.g., ACD or ACI models) in the literature, has also the advantage of greatly reducing the computational effort required when analysing UHF transaction data sets and of avoiding complex model specifications or obligatory deseasonalisation. We apply the LSFT to UHF FX series which are filtered by the directional change event and hence satisfy a scaling law. The scaling law relates the directional change duration in physical time (corresponding to one tick in intrinsic time) with the directional change threshold.

The structure of this paper is organised as follows. Section 2 motivates and introduces the methods employed in this study. Section 3 presents the empirical data and the results. Section 4 concludes.

2 Method

Our analysis is made in the frequency domain of an intrinsic-time process defined by a directional-change event. If the latter is governed by a scaling law, the filtered time series would have certain characteristics of scale-invariance and proportionality, even for its periodic patterns. In the following, Subsection 2.1 first describes the adopted event-based approach and the resulting scaling law. The LSFT for the spectral analysis of the UHF data is then introduced and defined in Section 2.2. Our goal is to capture the scale invariant periodicity of the intraday price series; i.e., for the same frequency in the spectral density of a directional change series sampled with a higher threshold, one can also find a corresponding significant peak in the spectral density sampled with a lower threshold - despite the irregular spacing in (physical) time.

2.1 Intrinsic Time and Directional Changes

Directional changes of price dynamics are the main source of volatility. Historically, the concept of directional change played an important role in technical analysis, as turning points of fundamental price movements are used by intraday traders to identify optimal times to buy or sell. For example, point-and-figure charting techniques, reportedly in use from the late 19th century, track price changes of fixed thresholds and significant price reversals, and are often employed to identify price trends, support and resistance levels in intraday trading data (among the oldest written references are Wyckoff, 1910 and deVilliers, 1933). Additionally, the so called "directional change frequency", which estimates the average number of directional price changes of a given threshold over a data sample, can be interpreted as an alternative measure of risk (Guillaume, Dacorogna, Davé, Müller, Olsen, and Pictet, 1997).

Let x denote the price and Δx the price change. In the event-driven setting

outlined above, the event is a directional change and its accompanied overshoot. More precisely, the absolute price change ("total price movement") Δx_{tm} between two local extremal values (minimum and maximum price) is decomposed into two sections: a fixed directional change threshold Δx_{dc} and a stochastic overshoot Δx_{os}, which represents the price movement beyond the fixed threshold. Such fixed event threshold defines the minimum price move between two consecutive local extrema and fully characterises the directional changes, which are computed iteratively from the last high or low, depending on whether the directional change is assumed to be downward or upward. At each iteration, the high is updated to the maximum between the current price and the last high, or the low to the minimum between the current price and the last low. At each occurrence of a directional-change event, the direction of the price move alternates, and the overshoot Δx_{os} associated with the previous directional change is determined *ex-post* as the difference between the last high or low and the price corresponding to that directional change. A price sample and its decomposition into directional-change and overshoot components are shown in Figure 1.

Let $\langle \cdot \rangle$ denote the average operator. Glattfelder, Dupuis, and Olsen (2011) have shown that the mean absolute price movement can be decomposed into a directional change and an overshoot, i.e. $\langle |\Delta x_{tm}| \rangle = \langle |\Delta x_{dc}| \rangle + \langle |\Delta x_{os}| \rangle$. The points in which the threshold is triggered, either upwards or downwards, are independent of the notion of physical time and form a series of directional-change events to be analysed using the LSFT. This event is chosen, not only because of (a) its scaling properties but also for (b) the "natural" periodic behaviour of FX markets due to their market microstructure effects (see, e.g., Lyons, 2001, or MacDonald, 2007).

Let Δt_{dc} denote the directional change duration, i.e. the elapsed time of a directional change of a price movement for a given threshold size. The directional change duration is measured in physical time and is stochastic; in intrinsic time it is measured in 'ticks' (Derman, 2002). The model applied here is the empirical scaling

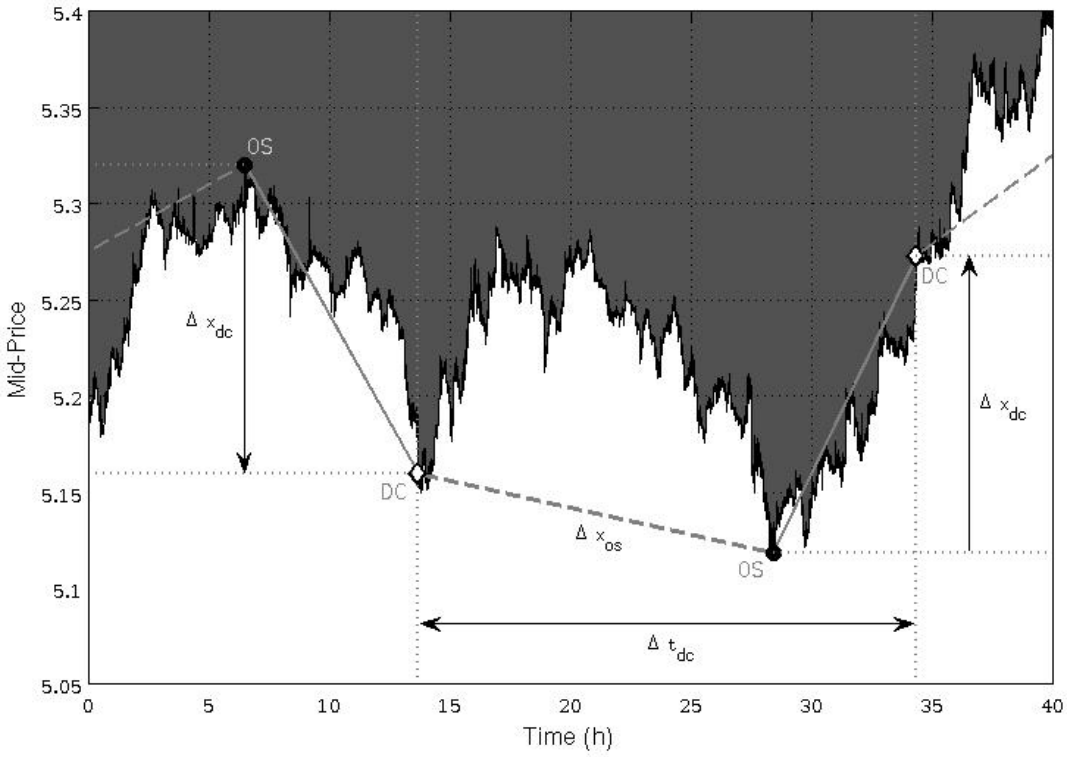

Figure 1: Dissection of mid-price curve into directional-change and overshoot sections. The graph shows a 40-hour by a threshold $\Delta x_{dc} = 3\%$ (currency pair: AUD-HKD). The directional-change events (diamonds) act as cut-off points, decomposing an absolute price change between a minimum and a maximum price (bullets) into directional-change Δx_{dc} (solid lines) and overshoot Δx_{os} (dashed lines) components. Intrinsic time ticks only at directional-change events, and the elapsing time between two contiguous events, i.e. the directional change duration, is denoted by Δt_{dc}.

law obtained by Glattfelder, Dupuis, and Olsen (2011) that describes

$$\langle \Delta t_{dc} \rangle = c(\Delta x_{dc})^k \quad , \tag{1}$$

where c is a constant and k is the scaling exponent. This scaling law describes the relationship between the average duration of directional changes (which is a random variable) and the size of a given price move threshold (which is pre-specified). By taking the logarithm of both sides of eq. (1), the power law relationship is cast into the linear equation

$$\log(\langle \Delta t_{dc} \rangle) = \log(c) + k \cdot \log(\Delta x_{dc}) \quad , \tag{2}$$

characterised by the slope k and the intercept $\log(c)$. The scaling exponent k measures the proportional change of the average directional-change duration due to an increment of the price threshold. Different directional-change threshold sizes $\Delta x_{dc} = \{10\text{bp}, 15\text{bp}, 20\text{bp}, 25\text{bp}, 30\text{bp}, 40\text{bp}, 50\text{bp}, 75\text{bp}, 100\text{bp}, 125\text{bp}, 150\text{bp}, 175\text{bp}, 200\text{bp}\}$ are chosen to generate the respective average directional-change durations for the individual sampling window. Standard linear OLS regression is used to estimate the scaling law parameters in eq. (2); the results are presented in Section 3.

The objective of this work is to demonstrate that the use of LSFT within an event-based framework reveals new periodic patterns in FX time series and provides insightful information on the price process with respect to different threshold levels and their corresponding seasonality. The cut-off points between each directional change and the corresponding overshoot form a new event-based and irregularly-spaced time series in intrinsic time (see Figure 1), which serves as input for the LSFT to calculate the spectral density function (SDF). The LSFT framework is described in the following section.

2.2 Spectral Analysis of Tick-Data

Spectral analysis decomposes a time series into its periodic frequencies in order to detect and analyse its cyclical behaviour. The application of spectral techniques in periodic economic processes has a long history, and a significant effort is employed in the estimation of the spectral density function (SDF) (Priestley, 1981). The SDF represents the analogue of the autocorrelation function in the time domain and encapsulates the frequency properties of the time series determining how the variation in a time series is built-up by components at different frequencies.

For standard periodic time series a FFT algorithm is generally employed to determine their spectral properties (Priestley, 1981). As tick-by-tick data and the resultant filtered time series in intrinsic time are unevenly-spaced, the traditional

FFT can not be applied without artificially tampering with the raw data (see also Dacorogna, Gençay, Müller, Olsen, and Pictet, 2001; Bauwens, Ben Omrane, and Giot, 2005; Ben Omrane and de Bodt, 2007). Attempts to transform the irregularly-spaced raw data into regularly-spaced data, by regular resampling, averaging, or using interpolation, prior to applying the FFT to calculate the SDF (e.g., Bisig, Dupuis, Impagliazzo, and Olsen, 2012), has recently been demonstrated to cause (a) loss of information, (b) generation of spurious data, or (c) both. It has also been shown that these limitations can be overcome using the LSFT (see Giampaoli, Ng, and Constantinou, 2009). Lomb (1976) first introduced this statistical method in astrophysics and fitted sinusoidal curves to the unevenly-spaced data by least-squares in order to determine their periodic behaviour, despite the irregular spacing in time. Scargle (1982) later developed the methodology further by deriving the standardised Lomb-Scargle (LS) periodogram that has well defined statistical properties as the work of Horne and Baliunas (1986) demonstrated.

Many diverse areas of science have tackled this issue using the robust framework of the LSFT (for an overview, see Ware, 1998). Under this framework, the data on the non-equally spaced grid is transformed into the frequency domain in order to obtain an unbiased estimation of the SDF. The resulting SDF is calculated for $k \in \{1, 2, 3..., M\}$ frequencies, with M chosen as outlined in Press, Flannery, Teukolsky, and Vetterling (1992). Consider a signal x, observed a time t_j, with mean $\bar{x}$ and variance σ_x. The normalised SDF is given by

$$SDF_{LS}(\omega_k) = \frac{1}{2\sigma_x^2} \left\{ \frac{\left[\sum_{j=1}^{N} (x_j - \bar{x}) \cos \omega_k (t_j - \tau)\right]^2}{\sum_{j=1}^{N} \cos^2 \omega_k (t_j - \tau)} + \frac{\left[\sum_{j=1}^{N} (x_j - \bar{x}) \sin \omega_k (t_j - \tau)\right]^2}{\sum_{j=1}^{N} \sin^2 \omega_k (t_j - \tau)} \right\} \quad (3)$$

and

$$\tau = \tau(\omega_k) = \frac{1}{2\omega_k} \arctan\left[\frac{\sum_{j=1}^{N} \sin(2\omega_k t_j)}{\sum_{j=1}^{N} \cos(2\omega_k t_j)}\right], \tag{4}$$

with $\omega_k = 2\pi f_k$ as the angular frequency (see also Press, Flannery, Teukolsky, and Vetterling, 1992, p. 581 for a modified version to increase the computational efficiency; a generalisation for the non-sinusoidal case can be found in Bretthorst, 2001). In addition, Scargle (1982, Appendix C) demonstrated that this particular choice of the offset τ makes eq. (3) identical to the expression obtained by linear least-squares fitting sine waves to the data (see also Van Dongen, Olofsen, Van Hartevelt, and Kruyt, 1999). Scargle (1982) has also shown that the LS periodogram has an exponential probability distribution with unit mean. The probability that SDF_{LS} will be between some positive quantity z and $z + dz$ is $e^{-z}dz$, and the probability of none of them give larger values than z is $(1 - e^{-z})^M$. Therefore, we can compute the false-alarm probability of the null hypothesis, e.g., the probability that a given peak in the periodogram is not significant, by $P(> z) \equiv 1 - (1 - e^{-z})^M$ (Press and Rybicki, 1989).

3 Empirical Data and Results

The tick-by-tick data set comprises 6 currency pairs spanning 3 months, from November 1, 2008 to January 31, 2009. The following currency pairs are considered (with the number of observations enclosed in brackets): AUD-HKD (4'472'222), AUD-JPY (18'821'980), EUR-JPY (32'250'932), EUR-USD (23'057'152), HKD-JPY (6'052'923), USD-JPY (19'010'622). The varying number of ticks is mostly due to the fact that different exchange rates have different degrees of liquidity (Glattfelder, Dupuis, and Olsen, 2011). The data set includes a bid, an ask price, a timestamp, and each time series is filtered as observations with the same timestamp are averaged

Currency	AUD-HKD	AUD-JPY	EUR-JPY	EUR-USD	HKD-JPY	USD-JPY
Threshold	$N(\Delta x_{dc})$ (DC/h)	$N(\Delta x_{dc})$ (DC/h)	$N(\Delta x_{dc})$ (DC/h)	$N(\Delta x_{dc})$ (DC/h)	$N(\Delta x_{dc})$ (DC/h)	$N(\Delta x_{dc})$ (DC/h)
10 bp	22425 (14.8363)	32313 (21.7158)	15557 (10.4550)	8154 (5.4831)	8564 (5.7606)	8573 (5.7614)
15 bp	10615 (7.0228)	15006 (10.0847)	7693 (5.1700)	3921 (2.6366)	3837 (2.5810)	3807 (2.5585)
20 bp	6289 (4.1608)	8947 (6.0128)	4601 (3.0921)	2300 (1.5466)	2270 (1.5269)	2241 (1.5061)
25 bp	4185 (2.7688)	5994 (4.0282)	3027 (2.0343)	1545 (1.0389)	1428 (0.9605)	1402 (0.9422)
30 bp	2962 (1.9596)	4390 (2.9503)	2157 (1.4496)	1084 (0.7289)	1023 (0.6881)	1009 (0.6781)
40 bp	1677 (1.1095)	2572 (1.7285)	1246 (0.8374)	622 (0.4183)	588 (0.3955)	578 (0.3884)
50 bp	1076 (0.7119)	1689 (1.1351)	793 (0.5329)	380 (0.2555)	379 (0.2549)	372 (0.2500)
75 bp	464 (0.3070)	754 (0.5067)	355 (0.2386)	175 (0.1177)	165 (0.1110)	162 (0.1089)
100 bp	251 (0.1661)	425 (0.2856)	188 (0.1263)	97 (0.0652)	87 (0.0585)	84 (0.0565)
125 bp	173 (0.1145)	267 (0.1794)	122 (0.0820)	57 (0.0383)	50 (0.0336)	49 (0.0329)
150 bp	121 (0.0801)	187 (0.1257)	84 (0.0565)	39 (0.0262)	30 (0.0202)	29 (0.0195)
175 bp	91 (0.0602)	133 (0.0894)	64 (0.0430)	27 (0.0182)	23 (0.0155)	22 (0.0148)
200 bp	67 (0.0443)	113 (0.0759)	54 (0.0363)	25 (0.0168)	19 (0.0128)	18 (0.0121)

Table 1: **Number of directional changes (time period: 11/2008 - 01/2009)** - The table shows for each given threshold Δx_{dc} the total number of directional changes $N(\Delta x_{dc})$, and the number of directional changes per hour (DC/h).

out. The following definition of mid-price is considered:

$$x_t = (bid_t + ask_t)/2. \tag{5}$$

From the raw data, a mid-price process for each of the currency pairs is obtained using eq. (5). It is the mid-price data which are filtered to obtain the intrinsic time series. The filtering follows the procedure outlined in Section 2.1, i.e. by decomposing the total price movements into directional-change (of thresholds $\Delta x_{dc} = \{$10bp, 15bp, 20bp, 25bp, 30bp, 40bp, 50bp, 75bp, 100bp, 125bp, 150bp, 175bp, 200bp$\}$) and overshoot sections. Table 1 shows, for each threshold Δx_{dc}, the number of

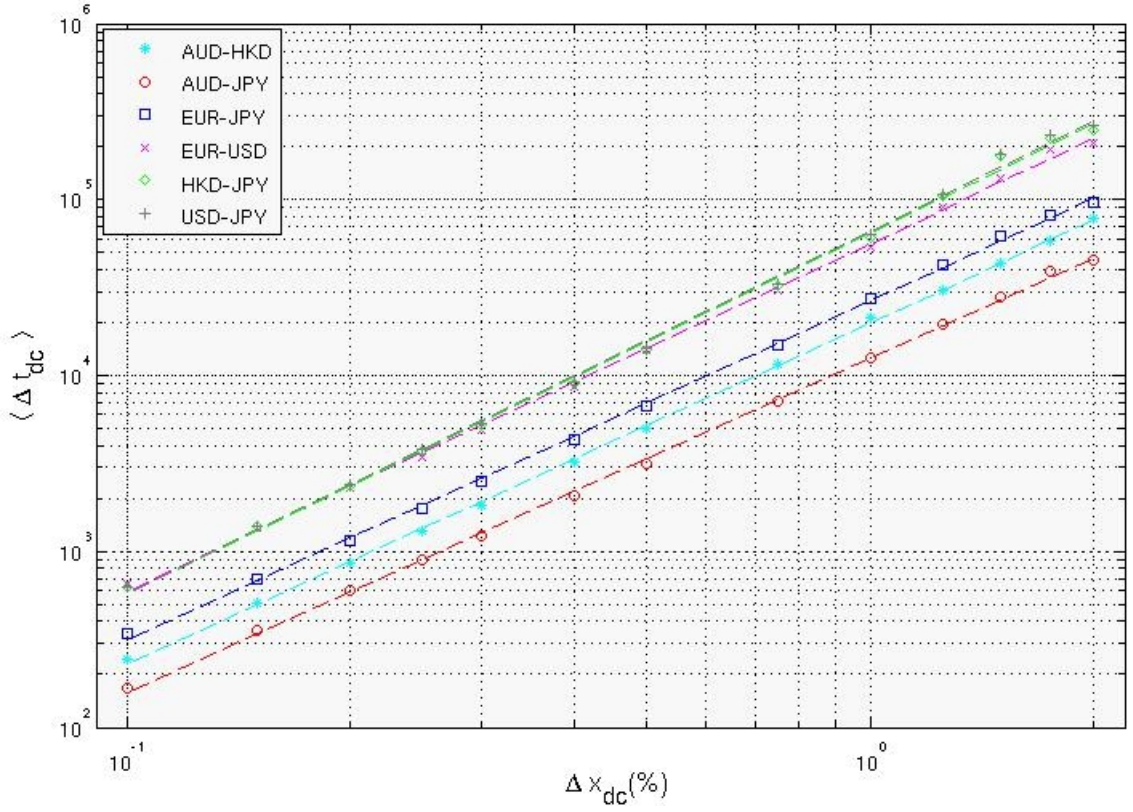

Figure 2: Empirical scaling law: estimated scaling law regression lines for the different currency pairs (time period: 11/2008 - 01/2009). The x-axis shows the threshold size as relative price change, and the y-axis the respective average time (in seconds), for a given threshold, to observe the reversion of the price move.

directional changes $N(\Delta x_{dc})$ and the "speed" of change of the mid-price process, measured in directional changes per hour (DC/h).

Figure 2 illustrates the power law regression (eq. 2) for the currency pairs considered in this paper. Table 2 lists the intercept, slope, associated R^2 and mean square error (MSE) statistics. For each of the currency pairs, we also show the results for a geometric Brownian motion (GBM), which we used as a benchmark. Given an initial mid-price x_0, the process generated is

$$x_t = x_0 \cdot e^{\left(\mu - \frac{\sigma^2}{2}\right)t + \sigma W_t}, \tag{6}$$

where $x_t \sim GBM(\mu, \sigma^2)$, W_t is a Wiener process, and μ and σ are estimated from the data. The regression coefficients for the GBM are obtained by averaging the

Currency	Intercept (s.e.)	Slope (s.e.)	R^2	MSE
AUD-HKD	8.1806 (0.0258)	1.9407 (0.0111)	0.9996	2.7E-4
GBM	5.9829 (0.0704)	1.7176 (0.0304)	0.9965	0.0021
AUD-JPY	7.8952 (0.0284)	1.8985 (0.0123)	0.9995	3.3E-4
GBM	5.6690 (0.0802)	1.6578 (0.0346)	0.9952	0.0027
EUR-JPY	8.2895 (0.0342)	1.9316 (0.0148)	0.9994	4.8E-4
GBM	6.1383 (0.0667)	1.7451 (0.0288)	0.9970	0.0019
EUR-USD	8.7042 (0.0445)	1.9768 (0.0192)	0.9990	8.2E-4
GBM	6.5774 (0.0578)	1.8115 (0.0249)	0.9978	0.0015
HKD-JPY	8.9131 (0.602)	2.0520 (0.0260)	0.9982	0.0015
GBM	6.5938 (0.0585)	1.8149 (0.0252)	0.9978	0.0015
USD-JPY	8.9539 (0.0604)	2.0656 (0.0260)	0.9983	0.0015
GBM	6.6002 (0.0585)	1.8158 (0.0252)	0.9978	0.0015

Table 2: **Empirical scaling law** - Estimated regression parameters (time period: 11/2008 - 01/2009). The scaling law relates the average time interval for directional changes of given thresholds to occur to the size of the thresholds. For each currency pair, the last two rows show the regression parameters and the corresponding standard errors of the benchmark geometric Brownian motion (GBM).

OLS estimates over a sufficiently high number of iterations, so as to ensure good convergence properties. The slope of the curves (the key parameter in the power-law) are close to those reported in Glattfelder, Dupuis, and Olsen (2011), with similar associated statistics. This similarity illustrates the remarkable robustness of the scaling law as the data used in this investigation are later than those employed by Glattfelder, Dupuis, and Olsen (2011). In particular, it is noted that all the currency pairs show power-law behaviour which is statistically different from the corresponding GBM at the 99% confidence level.

Following the data filtering, the dissection (cut-off) points between directional-change and overshoot sections generate a new irregularly-spaced time series of

directional-change events in intrinsic time; the LSFT is then applied to calculate the SDF. Since the LSFT relies on the assumption of weak-stationarity of the data, the DC mid-price series were detrended, taking into account the irregularity in spacing between two contiguous observations, and tested for stationarity prior to the estimation of the spectral density. The Augmented Dickey-Fuller (Dickey and Fuller, 1981) and Phillips-Perron (Phillips and Perron, 1988) unit root tests were applied to assess the stationarity of the data at different lags, assuming an autoregressive model for the (detrended) mid-price process.

Figures 3A, 3B, and 3C show examples of the SDFs of mid-price directional-change events (in the top panels) and the corresponding false-alarm probabilities (in the bottom panels) of the currency pair EUR-JPY for 3 different thresholds (0.5%, 0.75%, 1.5%). For a better comparison with the corresponding results for the remaining currency pairs (see Appendix), the spectral densities are normalised by the maximum of SDF_{LS}. 3A illustrates that all the significant peaks (for a significance level of 95%) are located in the left-hand side of the graph[2], i.e. that the highest contribution to the variance of the mid-price process comes from relatively low frequencies (corresponding to a period longer than 23 hours). On the other hand, Figures 3B and 3C illustrate that, as the directional-change threshold increases, the spectral density tends to shift further towards the left-hand side of the graph, that is towards the lower frequencies. All the significant peaks correspond in fact to periods longer than 138 and 824 hours, respectively for thresholds of 0.75% and 1.5%. This is perfectly consistent with the expectation that, as the directional-change threshold increases, the time needed to trigger that threshold also increases.

In particular, the scaling property of directional-change durations assures that in the frequency domain, periodicities associated with a particular threshold are replicated in the empirical spectral densities of directional-change events of those of lower thresholds. Table 3 ($\Delta x_{dc} = \{10\text{bp}, 15\text{bp}, 20\text{bp}\}$) and Table 4 ($\Delta x_{dc} =$

[2] The frequency axis was truncated below the median value, thereby excluding frequencies for which the spectral density was substantially lower than the significance level.

(A) EUR-JPY

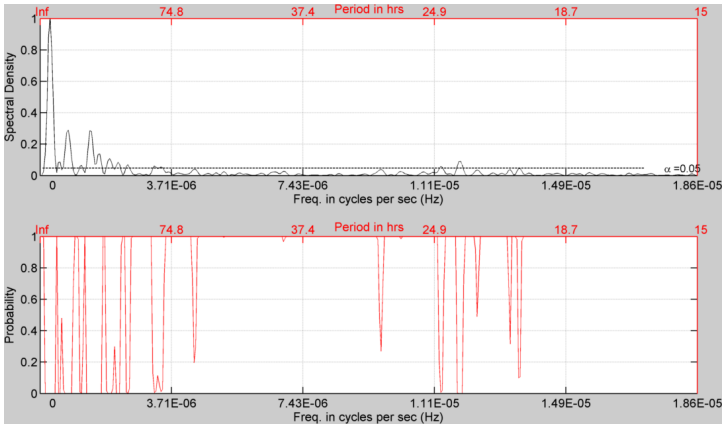

(B) EUR-JPY

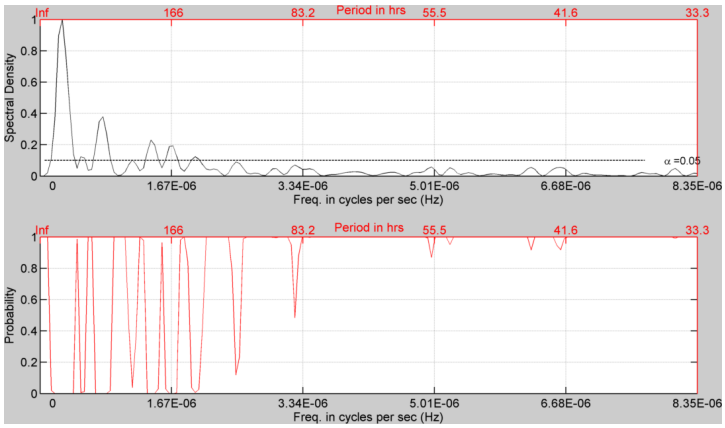

(C) EUR-JPY

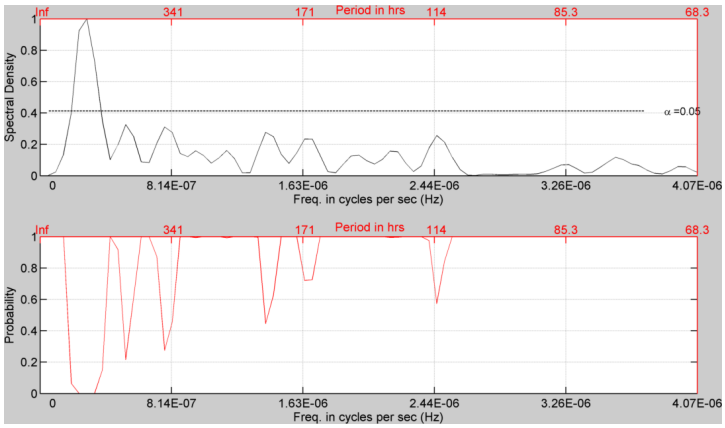

Figure 3: **Empirical spectral density of directional-change events and associated false alarm probabilities for EUR-JPY rate.** The upper panels show the empirical spectral densities (normalised) of mid-price directional change events for the thresholds 0.50% (3A), 0.75% (3B) and 1.5% (3C), respectively. The lower panel shows the corresponding false alarm probabilities of the estimated spectral density at 95% s.l. for a given frequency expressed in Hz. The associated period in hours is indicated in the secondary x-axis.

Threshold	AUD-HKD	AUD-JPY	EUR-JPY	EUR-USD	HKD-JPY	USD-JPY
20 bp	11.8697	11.8443	7.9351		10.2617	8.2999
	7.9392	11.3039			8.3098	6.1711
		7.9278			7.8178	6.0028
					6.9007	4.7771
					6.2940	
					6.0015	
					4.7761	
					3.9140	
					3.4909	
15 bp	11.8731	11.8445	11.8380	11.8587	8.2992	10.2461
	11.3385	11.3041	7.9341		7.3817	8.2999
	7.9414	10.9100			6.7989	6.0271
		7.9385			6.0266	
		7.8133			4.8154	
		5.9638				
		4.7720				
		3.9170				
10 bp	11.8732	11.8446	11.8650	11.8589	10.0204	10.0226
	11.3173	11.3042	10.3022	7.9323	9.2556	9.2721
	10.4739	10.9301	7.9364		8.3107	8.3125
	10.0724	7.9386	7.4772		6.9014	6.9109
	9.6695	7.8134	5.9622		6.0326	6.0278
	9.3119	7.4698	4.7746		5.9067	4.8164
	8.7207	5.9639	4.0192		5.1137	4.6145
	7.9415	5.5622			4.8153	3.2710
	7.8283	4.7721			4.6134	3.1648
	7.4888	4.6635			3.2721	
	7.1690	3.9170			3.1658	
	6.4636	2.6724				
	5.9718					
	5.0785					
	4.7812					
	4.0945					
	3.9192					
	3.1362					
	2.8096					
	2.1116					

Table 3: **Scaling property of directional-change durations for the currency pairs (time period: 11/2008 - 01/2009)** - The table lists for the three thresholds $\Delta x_{dc} = \{10\text{bp}, 15\text{bp}, 20\text{bp}\}$ a subsample of periods below 12 hours with significant peaks of the estimated spectral density at $> 95\%$ confidence level.

$\{25\text{bp}, 50\text{bp}, 75\text{bp}\}$) report for the selected thresholds the corresponding periods expressed in hours, associated with significant peaks of the estimated spectral density at the 99% significance level. It can be seen that the periodicities associated with the 150bp threshold (see 3C) are replicated in the spectral density of directional-

Threshold	AUD-HKD	AUD-JPY	EUR-JPY	EUR-USD	HKD-JPY	USD-JPY
75 bp	333.6198	328.9597	197.4176	168.1769		202.4595
	261.0938	197.3758				
	200.1719	123.3599				
	171.5759	80.0172				
	23.4576					
50bp	335.4352	330.3823	197.9385	236.5594	203.8477	203.6614
	251.5764	247.7868		179.2117	120.6445	120.5343
	194.7688	198.2294				72.9158
		123.8934				
		80.3633				
		63.2647				
25 bp	335.6498	330.3083	197.9252	246.7681	282.6001	282.5144
	251.7374	247.7312	80.2399	185.0761	197.8200	197.7601
	194.8934	198.1850	63.1676	24.4729	72.3732	73.2445
	125.8687	123.8656	25.7046		25.3615	24.5157
	81.6445	80.3453	23.3770		21.3475	21.3410
	61.0272	42.4682	20.9815		16.0395	
	42.2496	35.3902	11.8518		10.2497	
	37.7606	28.7225			4.7783	
	28.6336	25.8502			3.4909	
	25.8192	23.4077				
	24.5597	21.3102				
	23.4174	18.5220				
	21.0512	17.6426				
	11.8697	13.0959				
	11.314	11.8437				
		7.9380				

Table 4: **Scaling property of directional-change durations for the currency pairs (time period: 11/2008 - 01/2009)** - The table lists for the three thresholds $\Delta x_{dc} = \{25\text{bp}, 50\text{bp}, 75\text{bp}\}$ a subsample of periods below 336 hours (2 weeks) with significant peaks of the estimated spectral density at $> 95\%$ confidence level.

change events sampled with both the 75bp and 50bp thresholds (see 3B and 3C). Similarly, the additional periodicities associated with the 75bp threshold are again propagated in the 50bp threshold and so on. If we observe a 150bp price change about every 360 hours on average (see Table 3), for example, we should also observe a 75bp *and* a 50bp price change at each full cycle.[3] In other words, for the same frequency in the spectral density of a directional change series sampled with a higher threshold, one can also find a corresponding significant peak in the spectral density

[3]Differences in the values might occur as "rounding errors" as the periods are actually calculated as reciprocal values from the original frequencies that are expressed in Hz. As discernible in Table 3, the lower the reported period (i.e., the higher the estimated frequency), the smaller are the gaps between the values across the different thresholds.

sampled with a lower threshold - despite the irregular spacing in (physical) time. This remarkable behaviour in the frequency domain is due to the scaling properties in the time domain, and is evident for other thresholds for the EUR-JPY FX rate, as well as for the other currency pairs investigated in this study. This finding is not to be confused with the aliasing or masking effect in standard spectral analysis as we consider the time series in event time (all irregularly spaced in time and differently sampled depending on the threshold).

In general, similar conclusions can be drawn analysing a different currency pair. For example, the spectral density of the AUD-HKD mid-price (see Figure 5) exhibits periodicities similar to those of the corresponding SDF of the currency pair EUR-JPY, showing an analogous trend, as the period associated with the directional changes tends to get longer as the directional-change threshold increases. Results for the other FX pairs with similar implications are shown in the Appendix (see Figures 5 to 8).

Future research will focus on the application of the proposed approach in algorithmic trading: for example, once a significant periodic component with period τ has been detected for a given price p_0, a simple trading strategy could be devised whereby the agent takes a short or a long position on the asset held, if its current market price is, respectively, above or below the target price p_0, and closes the positions after time τ, or when the asset price reaches again the initial level p_0.

4 Conclusion

Ultra-high frequency (UHF) data are observed in real-time and therefore are characterised by the irregularity of time intervals between two consecutive events. This paper combines the Lomb-Scargle Fourier Transform (LSFT) and an event-based approach, to analyse foreign exchange tick-by-tick data. The LSFT implicitly takes into account the non-periodic property of UHF data without the need to first trans-

form the data to a periodic array. Using empirical transaction data from FX markets and adopting an event-based time scale (known as intrinsic time), the spectral analysis shows that various parts of the whole price process display different periodic patterns, revealed by the energy of the process in the respective frequency domain. The period associated with these patterns tends to increase as the directional-change threshold increases, confirming similar results in other studies (see e.g. Glattfelder, Dupuis, and Olsen, 2011).

Interestingly, the scaling property of directional-change durations in the time domain, has also notable repercussions in the frequency domain. In fact, if a price series is irregularly spaced in time, it can be filtered using a given DC threshold contains periodic components, which then can be detected in series filtered at lower thresholds. For the same frequency in the spectral density of a DC series sampled with a high threshold, one can also detect a corresponding peak, above the significance level, in the spectral density of prices sampled using a lower threshold. The same analysis extended to stochastic overshoots, exhibit a similar behaviour, thus implying the existence of equivalent periodic patterns in the frequency domain.

Further, by using a set of different directional-change thresholds, this event-setting allows us not only to model the behaviour of market agents with different risk preferences and dealing frequencies, but also to capture seasonal volatility patterns present in the data.

References

Aldridge, I. (2010): *High-Frequency Trading: A Practical Guide to Algorithmic Strategies and Trading Systems*. Wiley, 1 edn.

Bauwens, L., W. Ben Omrane, and P. Giot (2005): *Journal of International Money and Finance*24(7), 1108–1125.

Ben Omrane, W., and E. de Bodt (2007): "Using self-organizing maps to adjust for intra-day seasonality," *Journal of Banking & Finance*, 31(6), 1817–1838.

Bisig, T., A. Dupuis, V. Impagliazzo, and R. B. Olsen (2012): "The scale of market quakes," *Quantitative Finance*, 12(4), 501–508.

Bouchaud, J.-P. (2001): "Power laws in economics and finance: some ideas from physics," *Quantitative Finance*, 1(1), 105–112.

Bouchaud, J.-P. (2002): "An introduction to statistical finance," *Physica A: Statistical Mechanics and its Applications*, 313(1-2), 238–251.

Bretthorst, G. L. (2001): "Generalizing the Lomb-Scargle periodogram-the non-sinusoidal case," in *Bayesian Inference and Maximum Entropy Methods in Science and Engineering*, vol. 568, pp. 246–251.

Chordia, T., R. Roll, and A. Subrahmanyam (2001): "Market Liquidity and Trading Activity," *The Journal of Finance*, 56(2), 501–530.

Dacorogna, M. M., R. Gençay, U. A. Müller, R. B. Olsen, and O. V. Pictet (2001): *An Introduction to High-Frequency Finance*. Academic Press, 1 edn.

Derman, E. (2002): "The perception of time, risk and return during periods of speculation," *Quantitative Finance*, 2(4), 282–296.

deVilliers, V. (1933): *The Point and Figure Method of Anticipating Stock Prices: Complete Theory & Practice*. Windsor Books.

Dickey, D. A., and W. A. Fuller (1981): "Likelihood Ratio Statistics for Autoregressive Time Series with a Unit Root," *Econometrica*, 49(4), 1057–72.

Giampaoli, I., W. L. Ng, and N. Constantinou (2009): "Analysis of ultra-high-frequency financial data using advanced Fourier transforms," *Finance Research Letters*, 6(1), 47–53.

Glattfelder, J. B., A. Dupuis, and R. B. Olsen (2011): "Patterns in high-frequency FX data: discovery of 12 empirical scaling laws," *Quantitative Finance*, 11(4), 599–614.

Guillaume, D. M., M. M. Dacorogna, R. R. Davé, U. A. Müller, R. B. Olsen, and O. V. Pictet (1997): "From the bird's eye to the microscope: A survey of new stylized facts of the intra-daily foreign exchange markets," *Finance and Stochastics*, 1(2), 95–129.

Hautsch, N. (2004): *Modelling Irregularly Spaced Financial Data*. Springer, Heidelberg.

Horne, J. H., and S. L. Baliunas (1986): "A prescription for period analysis of unevenly sampled time series," *Astrophysical Journal*, 302, 757–763.

Lomb, N. R. (1976): "Least-squares frequency analysis of unequally spaced data," *Astrophysics and Space Science*, 39, 447–462.

Lyons, R. K. (2001): *The Microstructure Approach to Exchange Rates*. MIT Press, Cambridge, Mass.

MacDonald, R. (2007): *Exchange Rate Economics: Theories and Evidence*. Routledge, London.

Mandelbrot, B., and H. M. Taylor (1967): "On the distribution of stock prices differences," *Operations Research*, 15(6), 1057–1062.

Phillips, P. C. B., and P. Perron (1988): "Testing for a unit root in time series regression," *Biometrika*, 75(2), 335–346.

Press, W. H., B. P. Flannery, S. A. Teukolsky, and W. T. Vetterling (1992): *Numerical Recipes in C: The Art of Scientific Computing*. Cambridge University Press, 2 edn.

Press, W. H., and G. B. Rybicki (1989): "Fast algorithm for spectral analysis of unevenly sampled data," *Astrophysical Journal*, 338, 277–280.

Priestley, M. B. (1981): *Spectral Analysis and Time Series. Volume 1: Univariate Series.* Academic Press, 1st edn.

Scargle, J. D. (1982): "Studies in astronomical time series analysis. II - Statistical aspects of spectral analysis of unevenly spaced data," *Astrophysical Journal*, 263, 835–853.

Van Dongen, H., E. Olofsen, J. Van Hartevelt, and E. Kruyt (1999): "A Procedure of Multiple Period Searching in Unequally Spaced Time-Series with the Lomb-Scargle Method," *Biological Rhythm Research*, 30, 149–177.

Ware, A. F. (1998): "Fast Approximate Fourier Transforms for Irregularly Spaced Data," *SIAM Review*, 40, 838–856.

Wyckoff, R. D. (1910): *Studies in tape reading.* The Ticker Publishing Company, New York.

Appendix

(A) EUR-USD

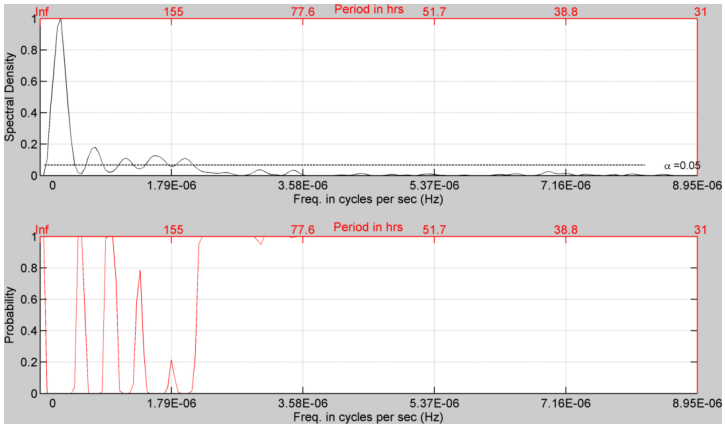

(B) EUR-USD

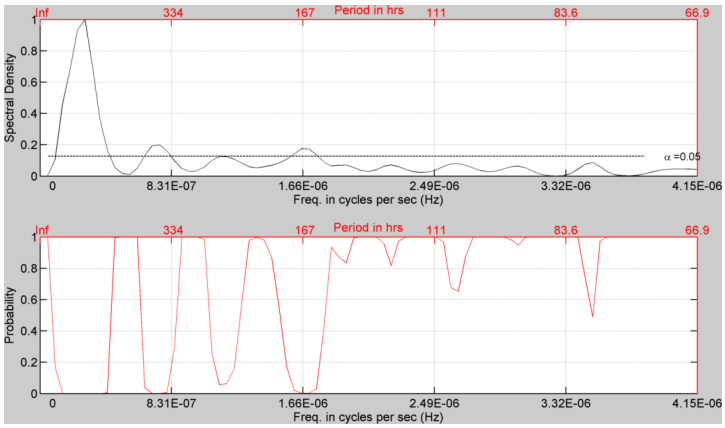

(C) EUR-USD

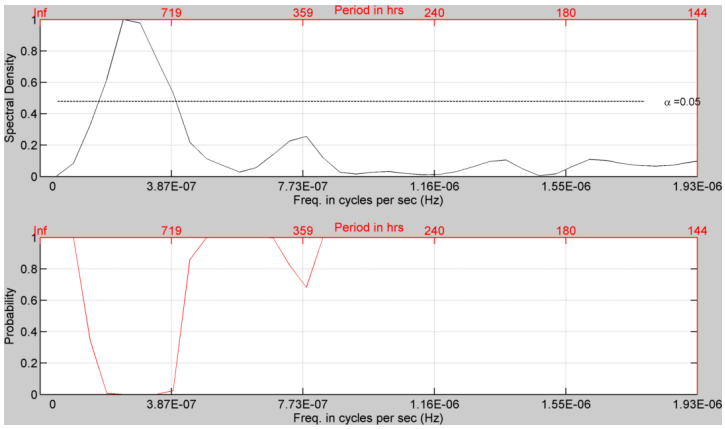

Figure 4: **Empirical spectral density of directional-change events and associated false alarm probabilities for EUR-USD rate.** The upper panels show the empirical spectral densities (normalised) of mid-price directional change events for the thresholds 0.50% (4A), 0.75% (4B) and 1.5% (4C), respectively. The lower panel shows the corresponding false alarm probabilities of the estimated spectral density at 95% s.l. for a given frequency expressed in Hz. The associated period in hours is indicated in the secondary x-axis.

(A) Threshold = 0.50%

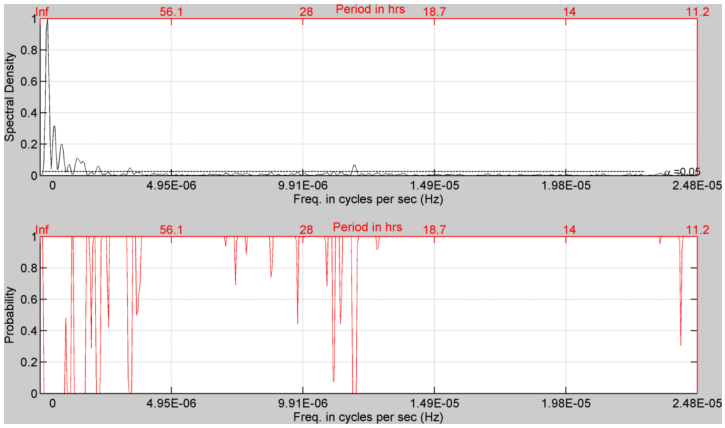

(B) Threshold = 0.75%

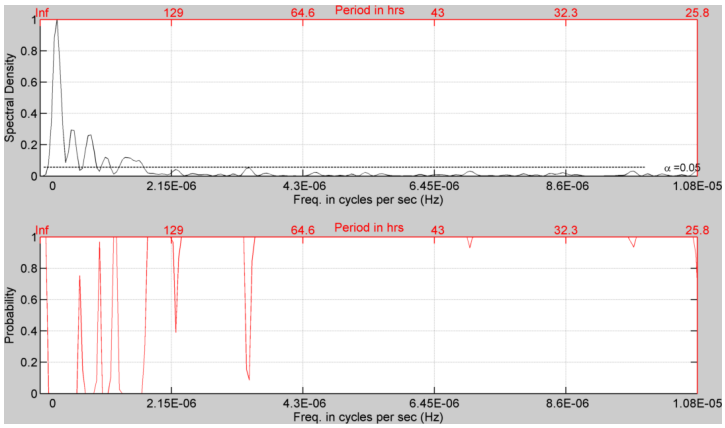

(C) Threshold = 1.5%

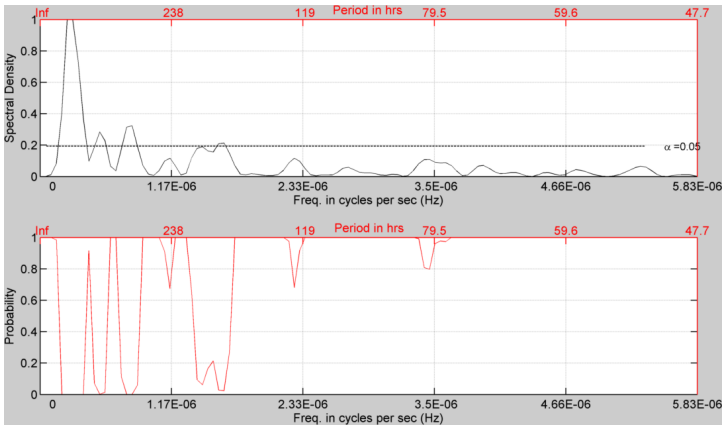

Figure 5: **Empirical spectral density of directional-change events and associated false alarm probabilities for AUD-HKD rate.** The upper panels show the empirical spectral densities (normalised) of mid-price directional change events for the thresholds 0.50% (**??**), 0.75% (5B) and 1.5% (5C), respectively. The lower panel shows the corresponding false alarm probabilities of the estimated spectral density at 95% s.l. for a given frequency expressed in Hz. The associated period in hours is indicated in the secondary x-axis.

(A) Threshold = 0.50%

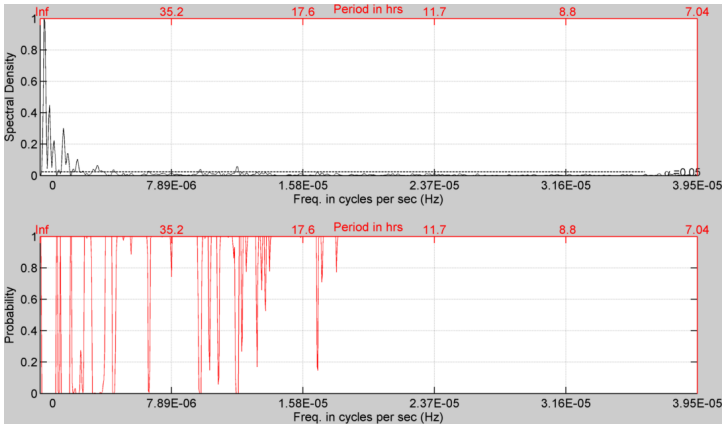

(B) Threshold = 0.75%

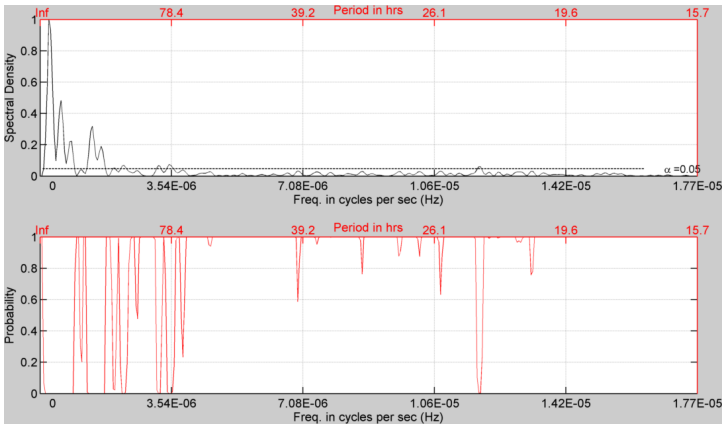

(C) Threshold = 1.5%

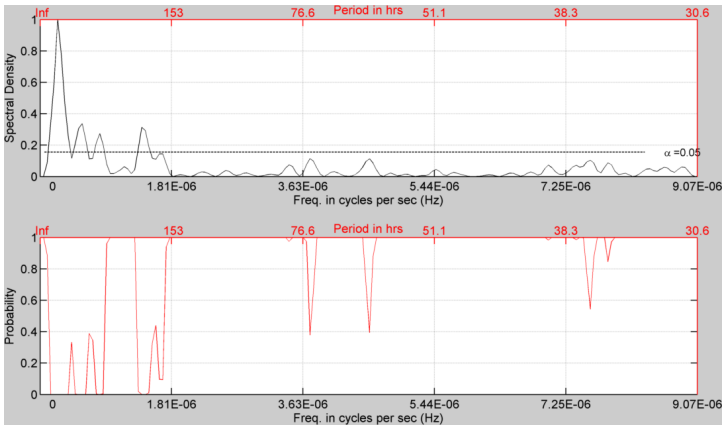

Figure 6: **Empirical spectral density of directional-change events and associated false alarm probabilities for AUD-JPY rate.** The upper panels show the empirical spectral densities (normalised) of mid-price directional change events for the thresholds 0.50% (6A), 0.75% (6B) and 1.5% (6C), respectively. The lower panel shows the corresponding false alarm probabilities of the estimated spectral density at 95% s.l. for a given frequency expressed in Hz. The associated period in hours is indicated in the secondary x-axis.

(A) Threshold = 0.50%

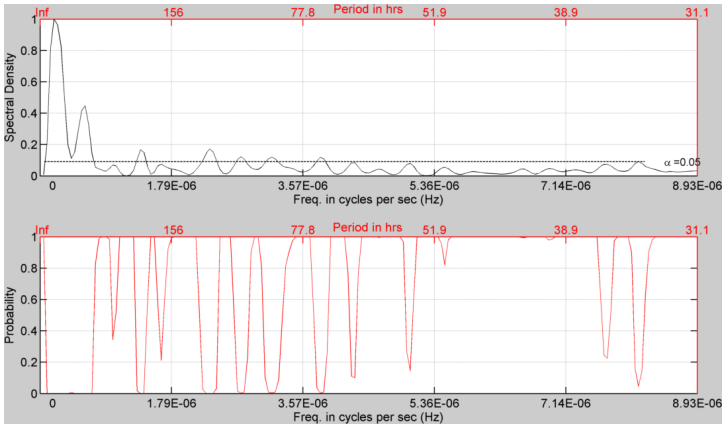

(B) Threshold = 0.75%

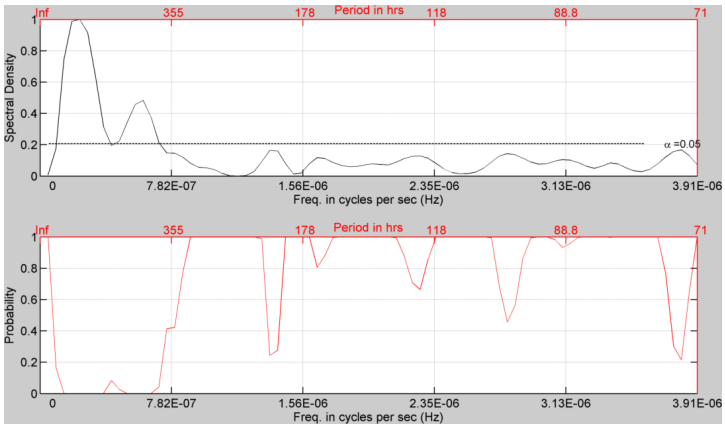

(C) Threshold = 1.5%

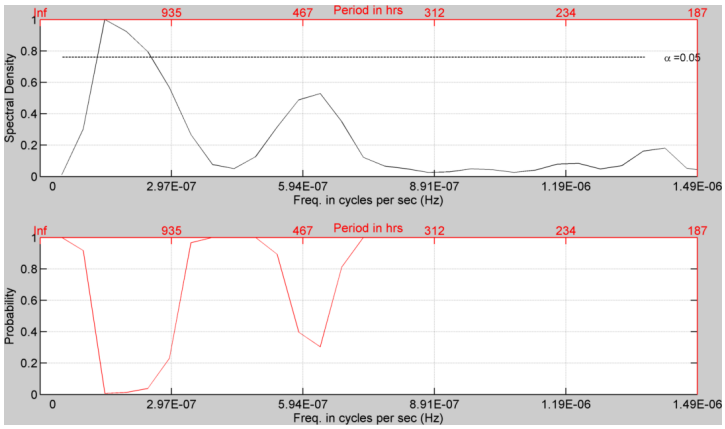

Figure 7: **Empirical spectral density of directional-change events and associated false alarm probabilities for HKD-JPY rate.** The upper panels show the empirical spectral densities (normalised) of mid-price directional change events for the thresholds 0.50% (7A), 0.75% (7B) and 1.5% (7C), respectively. The lower panel shows the corresponding false alarm probabilities of the estimated spectral density at 95% s.l. for a given frequency expressed in Hz. The associated period in hours is indicated in the secondary x-axis.

(A) Threshold = 0.50%

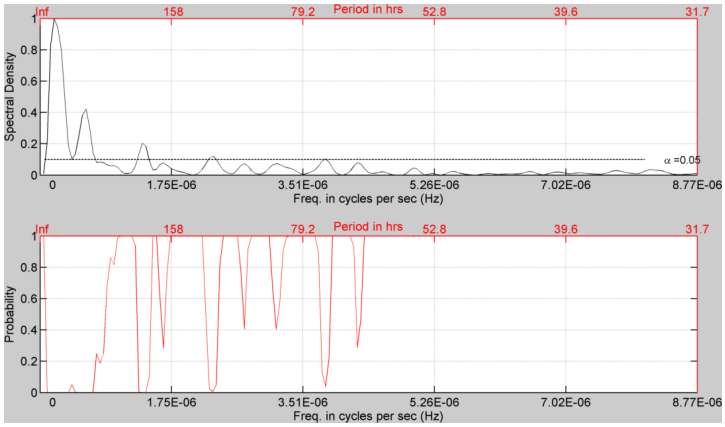

(B) Threshold = 0.75%

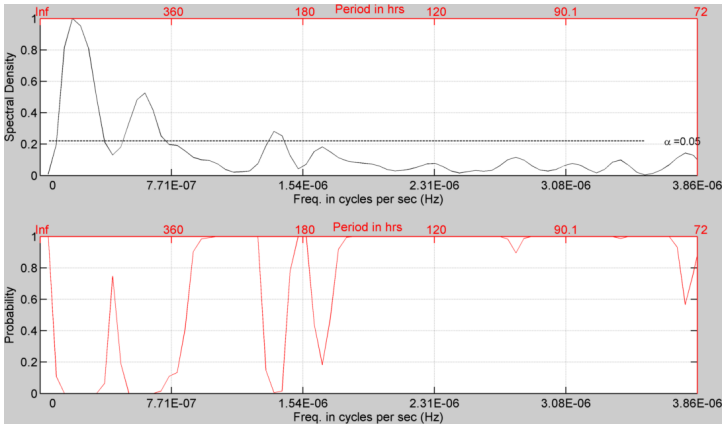

(C) Threshold = 1.5%

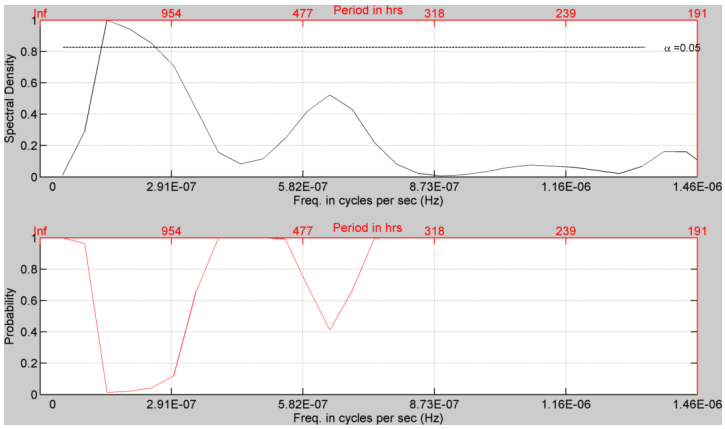

Figure 8: **Empirical spectral density of directional-change events and associated false alarm probabilities for USD-JPY rate.** The upper panels show the empirical spectral densities (normalised) of mid-price directional change events for the thresholds 0.50% (8A), 0.75% (8B) and 1.5% (8C), respectively. The lower panel shows the corresponding false alarm probabilities of the estimated spectral density at 95% s.l. for a given frequency expressed in Hz. The associated period in hours is indicated in the secondary x-axis.